



NASA TN D-2811

FACILITY FORM 602

N65-23690
(ACCESSION NUMBER)

21
(PAGES)

(NASA CR OR TMX OR AD NUMBER)

(THRU) _____

(CODE) _____

(CATEGORY) 01

**ZERO-LIFT DRAG AT MACH 1.42,
1.83, AND 2.21 OF A SERIES OF
WINGS WITH VARIATIONS OF
THICKNESS RATIO AND CHORD**

by Barrett L. Shrout

*Langley Research Center
Langley Station, Hampton, Va.*

GPO PRICE \$ _____
CFST1
~~GPO~~ PRICE(S) \$ 1.00

Hard copy (HC) _____
Microfiche (MF) 0.50

ZERO-LIFT DRAG AT MACH 1.42, 1.83, AND 2.21 OF A SERIES OF
WINGS WITH VARIATIONS OF THICKNESS RATIO AND CHORD

By Barrett L. Shroul

Langley Research Center
Langley Station, Hampton, Va.

NATIONAL AERONAUTICS AND SPACE ADMINISTRATION

ZERO-LIFT DRAG AT MACH 1.42, 1.83, AND 2.21 OF A SERIES OF
WINGS WITH VARIATIONS OF THICKNESS RATIO AND CHORD

By Barrett L. Shrout
Langley Research Center

SUMMARY

23690

A series of wing configurations having various spanwise distributions of chord and thickness ratio but having the same effective thickness ratio was subjected to both a theoretical and experimental investigation of the zero-lift drag characteristics in the Mach number range from 1.2 to 2.2. Semispan models of the wings were tested in the Langley 4- by 4-foot supersonic pressure tunnel at Mach numbers of 1.42, 1.83, and 2.21 and a Reynolds number per foot of 4.3×10^6 . Results of this experimental investigation were in good agreement with the theoretical data, and indicate that the chord and thickness distributions may be arranged in such a manner as to provide higher wing volume without a wave drag penalty. An extension of the theoretical analysis indicated that the wave drag of a wing can be significantly affected by relatively minor changes in planform.

Author

INTRODUCTION

In the development of supersonic aircraft, the consideration of wave drag has led to the use of wings with low thickness ratios, and has therefore resulted in problems of both structural design and relatively small wing volumes. Several experimental investigations have been made to determine the effectiveness of various approaches to the solution of the problem of increasing wing volume without inducing an increase in wave drag. Much of the work was concerned with variations in wing planform and wing thickness, particularly in the inboard regions of the wing. Some of the results of these investigations are presented in references 1 to 4.

Reference 5 presents some of the aerodynamic characteristics at Mach number 2.03 of two families of wings having systematic variations of chord and thickness ratio. The results indicate that as wing volume is concentrated inboard, particularly when in conjunction with a lengthening of the inboard wing chords, zero-lift wave drag is reduced although total volume is increased. The development process for the families of wings in reference 5 produced planforms with complex leading-edge sweep which varied from considerably more to slightly less than the sweep of the basic wing. Drag, as affected by Mach number, might therefore differ significantly within these families of wings so as to preclude a valid comparison through consideration of a single supersonic Mach number.

Theoretical studies of one of the wing families over the Mach number range from 1.2 to 2.2 were therefore conducted. To validate the theoretical analysis, experimental data were obtained at Mach numbers of 1.42, 1.83, and 2.21. Additional theoretical work directed toward exploring planform and sweep effects as produced by a systematic longitudinal shearing of the chords of the complex planform was also conducted. Results of these theoretical analyses and experimental tests are presented in the present paper.

SYMBOLS

b	wing span
c	local chord
C_D	drag coefficient, $\frac{\text{Drag}}{qS}$
$C_{D,W}$	zero-lift wave drag coefficient
$C_{D,o}$	zero-lift drag coefficient
M	Mach number
q	free-stream dynamic pressure
R	Reynolds number
S	wing area
t	local wing thickness
$(t/c)_e$	effective thickness ratio
V	volume of wing
y	dimension in spanwise direction with origin at wing root
Subscripts:	
adj	adjusted
max	maximum

MODELS

The basic family of wings considered in the theoretical analysis and tested in the wind tunnel consisted of five wings. Planform area, span, aspect ratio,

and midchord sweep are the same within the basic family. All the wings have an effective thickness ratio of 0.04, where effective thickness ratio is

$$\left(\frac{t}{c}\right)_e = \sqrt{\frac{\int_0^{b/2} \left(\frac{t}{c}\right)^2 c \, dy}{\int_0^{b/2} c \, dy}}$$

as derived in reference 5. Sketches of the basic wing family are shown in figure 1 and some of the geometric characteristics of the models are listed in table I.

Details of the generation of the wings of the family are given in reference 5. Hence, it should suffice to describe the development of the family of wings as follows: Wing I has a constant thickness ratio of 0.04; wing II has the planform of wing I and was produced by halving the tip-thickness ratio of wing I and imposing a parabolic spanwise variation of thickness ratio; wing III was produced by making its chord distribution proportional to the thickness distribution of wing II and its thickness distribution proportional to the chord distribution of wing II; wing IV was developed by imposing a constant thickness ratio of 0.04 on the wing III planform; and wing V has the same planform as wings III and IV and was generated by halving the tip thickness of wing IV and imposing a parabolic spanwise thickness ratio distribution.

Spanwise development of thickness ratio and volume for the wings is shown in figure 2. Circular-arc airfoil sections were used in all wings of the series.

APPARATUS AND TEST CONDITIONS

A sketch of the wing installation in the tunnel is shown in figure 3. All the wings are semispan models and were mounted by means of a stub at the wing root to a four-component, strain-gage balance located within a horizontal boundary-layer bypass plate, as shown schematically in the figure. A minimal clearance of 0.010 to 0.020 inch was provided between the wing root and the surface of the boundary-layer bypass plate.

The experimental investigation was performed in the Langley 4- by 4-foot supersonic pressure tunnel at Mach numbers of 1.42, 1.83, and 2.21 at a Reynolds number per foot of 4.3×10^6 . This same Reynolds number was used in the wind-tunnel tests of these wings at a Mach number of 2.03, reported in reference 5. In the present investigation the stagnation temperature was 110° F and the dew-point was maintained sufficiently low to prevent any significant condensation effects in the test section.

Transition of the boundary layer was fixed on the wings by 1/8-inch-wide strips of sparsely distributed carborundum grit located 1/4 inch downstream of the wing leading edge. For the tests at Mach number 1.42, No. 80 grit was used, whereas for the tests at Mach numbers 1.83 and 2.21, No. 60 grit was used. Drag data at zero lift were taken over a wide range of Reynolds numbers to insure that transition was fixed at the test Reynolds number. The wings were optically set at an angle of attack of 0° through the use of prisms recessed in the wing surface.

The accuracy of the data is estimated to be within the following limits:

M	±0.03
C _D	±0.0003

RESULTS AND DISCUSSION

Analysis of Theoretical and Experimental Data

The results of the theoretical analysis of the wave drag characteristics for the various wings of the basic series are shown in figure 4, with zero-lift wave drag coefficient plotted as a function of Mach number. The method of calculation is that of reference 6, and involves the solution of the von Kármán slender-body formula by means of a computer program. The theoretical wave drag coefficients for each wing were computed for Mach numbers from 1.2 to 2.2 in increments of about 0.2.

The theoretical data at the higher Mach numbers show the advantages of judicious variation of chord and thickness ratio to produce a higher wing volume without a wave drag penalty; in particular, wings IV and V, which have the highest volumes of the series, have the lowest wave drag coefficients. At the lower Mach numbers, there is a considerable variation in the levels of wave drag for the various wings. In comparison with the other wings, wing III, for example, has a low wave drag level in the lower Mach number range. This variation of wave drag coefficient with Mach number is discussed further in conjunction with the analysis of the experimental data.

Figure 5 shows typical plots of zero-lift drag coefficient as a function of Reynolds number for wings I and IV. The theoretical curves, shown for comparison, were obtained by using the wave drag coefficients in figure 4 and the skin-friction drag coefficients based on fully turbulent flow and calculated by the T' method of Sommer and Short (ref. 7). Flow over the wings was considered to be essentially fully turbulent at the test Reynolds number per foot of 4.3×10^6 .

Figure 6 shows a plot of zero-lift drag coefficient as a function of Mach number for all five wings of the basic family. The data for Mach numbers 1.42, 1.83, and 2.21, and the data from reference 5 for Mach number 2.03 are shown. The theoretical curves were obtained by using the same methods as were used for the theoretical curves in figure 5. The agreement between theory and experiment

is good, especially in view of the fact that the theory used in estimating the wave drag is based on the assumption that the shape to be evaluated may be represented by a series of reasonably slender equivalent bodies of revolution; and wings, such as those in the series reported herein, represent a rather severe departure from that assumption. A small increment of grit drag is probably present in the drag data. However, this increment is believed to fall within the accuracy limits of the test data and, consequently, no attempt has been made to correct for grit drag. It should be noted that the experimental data are consistently higher than the theoretical data, and that any correction made for grit drag would enhance the agreement between theory and experiment. In addition, because the grit-drag increment for wings of identical planform would be essentially constant, valid comparisons of the data of such wings, uncorrected for grit drag, can be made.

The experimental zero-lift drag data for the various wings were reduced by the corresponding estimated turbulent skin-friction coefficients to obtain the experimental wave drag coefficients for each wing at the various Mach numbers. These wave drag coefficients are presented in figure 7. At Mach numbers of 1.83 and 2.21, the trend is the same as that noted in the results of the tests at Mach number 2.03; that is, as the wing volume is concentrated inboard, particularly in conjunction with a lengthening of the inboard chords, wave drag is progressively reduced. However, a noticeable difference in the trend occurs at Mach number 1.42. For wings II and IV, there appears to be a slight penalty in wave drag, associated with concentration of volume at the inboard portion of the wing. With the exception of wing V, essentially the same results may be seen in figure 4 for the theoretical analysis at this Mach number. The reduction in drag level shown for wing III at Mach number 1.42, however, is not so pronounced in the experimental data as in the theoretical data. Note that wing III has an inverse taper in thickness ratio (very low values of thickness ratio inboard and high values outboard). It therefore represents an even more severe departure from the assumptions used in the method of theoretical analysis, and this fact may account for the discrepancy between theory and experiment at a Mach number of 1.42.

No volume constraint was applied in the generation of the wings of the family, and a considerable variation in total volume occurred. Because a large wing volume is desired for structural and fuel-storage purposes, it should be of interest to compare the wave drag levels of the wings on the basis of equal volume. By using the method in reference 5, the wave drag of each wing of the series was adjusted by a factor relating the volume of each wing to the volume of wing V, which is the wing of largest volume. In this method of adjustment, the wing area and planform are held constant and the volume change is accomplished by varying the effective thickness ratio. The adjusted wave drag coefficient becomes

$$(C_{D,W})_{adj} = C_{D,W} \left(\frac{V_{max}}{V} \right)^2$$

The values of adjusted wave drag coefficient, obtained by using this equation, are shown in figure 8. When compared on the basis of equal volume, the wings

with the long inboard elements and thickened roots show significant advantages in wave drag.

Extension of Theoretical Analysis

Because the theoretical method of analyzing drag gave results that were in good agreement with experimental data, this method was further utilized in analyzing the theoretical zero-lift wave drag characteristics of two series of wings derived from the original wing family. The planforms of these two series of wings (fig. 9) were generated by shearing the chords of the planform of wing III in such a manner that planform A has the same leading-edge sweep as wing I of the original series; planform B has the same quarter-chord sweep as wing I; planform C has the same three-quarter chord sweep as wing I; and planform D has the same trailing-edge sweep as wing I. The thickness distributions of wing IV and of wing V of the original family were imposed on these planforms. The geometric characteristics of area, aspect ratio, and span were the same as for the original family.

Figure 10 shows the results of the theoretical analysis of the two derived wing series - that is, the series with the thickness distribution of wing IV and the series with the thickness distribution of wing V. The theoretical wave drag curves for the original wings of both series (wings IV and V) are also plotted. In general, the wave drag tends to decrease with increasing Mach number for all the wings up to about Mach number 2.0. Above this Mach number, the drag level for wing A of both series increases slightly whereas the wave drag for the other wings continues to decrease or remains constant. The significant factor, however, is the progressive decrease in wave drag at any Mach number as the chords outboard of the root are sheared further rearward - that is, as each series progresses from wing A to wing D. This trend is not unexpected because, in the progression from planform A to planform D, the overall length of the wing increases and the equivalent bodies of revolution in the series representing the wing tend to be more slender; thus, in general, wave drag should decrease.

The results of this theoretical analysis should not be interpreted to mean that wing D of each series is necessarily the optimum wing, because other factors, such as the stability characteristics and structural suitability, must be considered. The illustration intended is that relatively minor changes in planform can materially affect the wave drag of the wing.

CONCLUDING REMARKS

The technique of attaining higher wing volumes without a serious wave drag penalty through concentration of volume inboard, particularly in conjunction with a lengthening of the inboard chords, has been shown to be valid within the Mach number range from 1.42 to 2.21. A series of wings having various spanwise distributions of thickness ratio and chord but having the same effective thickness ratio was subjected to both a theoretical and experimental investigation of zero-lift drag characteristics in the Mach number range from 1.2 to 2.2. Tests of semispan models of the wings were conducted in the Langley 4- by 4-foot

supersonic pressure tunnel at Mach numbers of 1.42, 1.83, and 2.21 at a Reynolds number per foot of 4.3×10^6 , and the results were in good agreement with the theoretical data.

Application of the theoretical method of analysis to two series of wings derived from the original family indicates that the wave drag of the wing can be substantially affected by relatively minor changes in planform.

Langley Research Center,
National Aeronautics and Space Administration,
Langley Station, Hampton, Va., February 19, 1965.

REFERENCES

1. Cooper, Morton; and Sevier, John R., Jr.: Effects of a Series of Inboard Plan-Form Modifications on the Longitudinal Characteristics of Two 47° Sweptback Wings of Aspect Ratio 3.5, Taper Ratio 0.2, and Different Thickness Distributions at Mach Numbers of 1.61 and 2.01. NACA RM L53E07a, 1953.
2. Sevier, John R., Jr.: Effects of a Series of Inboard Plan-Form Modifications on the Longitudinal Characteristics of Two Unswept Wings of Aspect Ratio 3.5, Taper Ratio 0.2, and Different Thickness Distributions at Mach Numbers of 1.61 and 2.01. NACA RM L53K11, 1954.
3. Bielat, Ralph P.; Harrison, Daniel E.; and Coppolino, Domenic A.: An Investigation at Transonic Speeds of the Effects of Thickness Ratio and of Thickened Root Sections on the Aerodynamic Characteristics of Wings With 47° Sweepback, Aspect Ratio 3.5, and Taper Ratio 0.2 in the Slotted Test Section of the Langley 8-Foot High-Speed Tunnel. NACA RM L51I04a, 1951.
4. Henning, Allen B.: Effects of Wing Inboard Plan-Form Modifications on Lift, Drag, and Longitudinal Stability at Mach Numbers From 1.0 to 2.3 of a Rocket-Propelled Free-Flight Model With a 52.5° Sweptback Wing of Aspect Ratio 3. NACA RM L57D29, 1957.
5. Robins, A. Warner; Harris, Roy V., Jr.; and Jackson, Charlie M., Jr.: Characteristics at Mach Number of 2.03 of a Series of Wings Having Various Spanwise Distributions of Thickness Ratio and Chord. NASA TN D-631, 1960.
6. Harris, Roy V., Jr.: An Analysis and Correlation of Aircraft Wave Drag. NASA TM X-947, 1964.
7. Sommer, Simon C.; and Short, Barbara J.: Free-Flight Measurements of Turbulent-Boundary-Layer Skin Friction in the Presence of Severe Aerodynamic Heating at Mach Numbers From 2.8 to 7.0. NACA TN 3391, 1955.

TABLE I
 GEOMETRIC CHARACTERISTICS OF MODELS

[All values correspond to full-span wing]

Model	Wing area, sq ft	Wing span, in.	Mean geometric chord, in.	Root chord, in.	Tip chord, in.	Root thickness ratio	Tip thickness ratio	Aspect ratio	Midchord sweep, deg	Leading-edge sweep, deg
I	1.60	24.0	11.022	16.000	3.200	0.0400	0.0400	2.5	55.71	63.44
II	1.60	24.0	11.022	16.000	3.200	.0607	.0200	2.5	55.71	63.44
III	1.60	24.0	14.311	25.492	1.681	.0237	.0720	2.5	55.71	Complex
IV	1.60	24.0	14.311	25.492	1.681	.0400	.0400	2.5	55.71	Complex
V	1.60	24.0	14.311	25.492	1.681	.0545	.0200	2.5	55.71	Complex

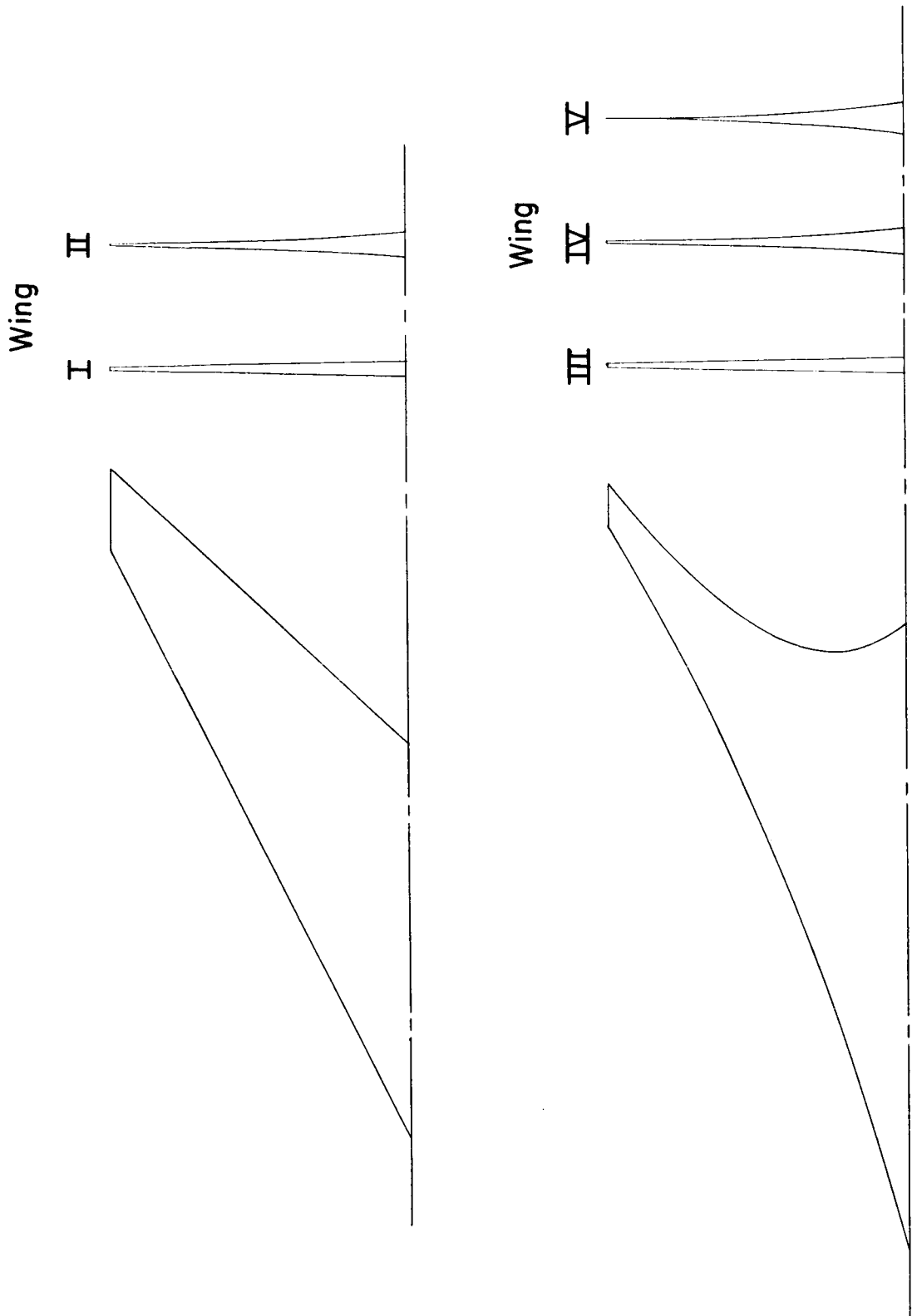


Figure 1.- Sketches of the wing semispans.

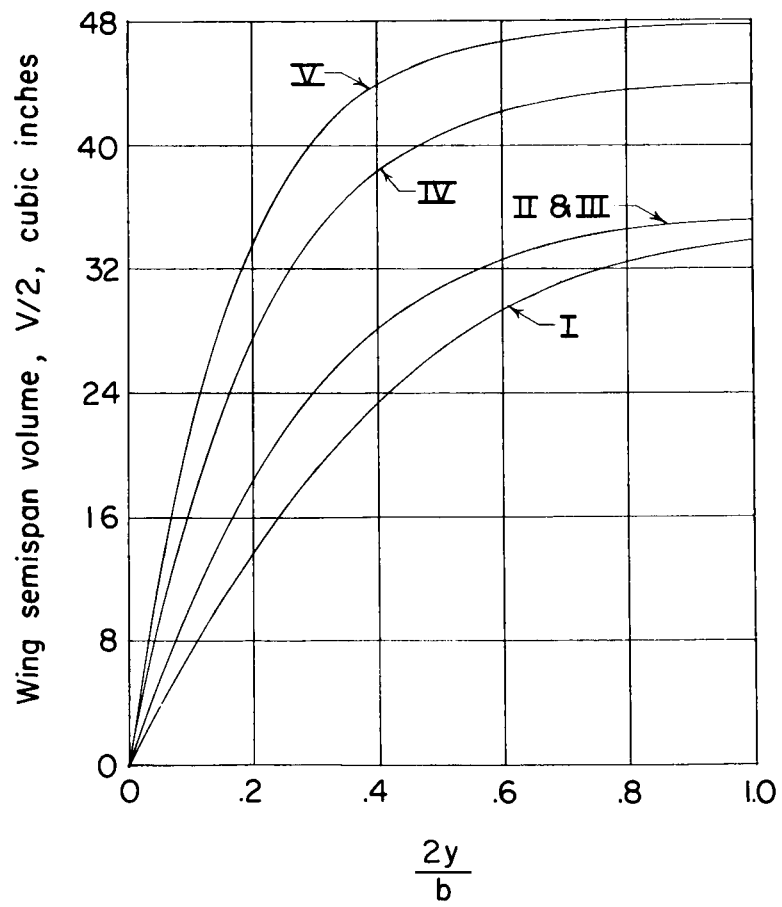
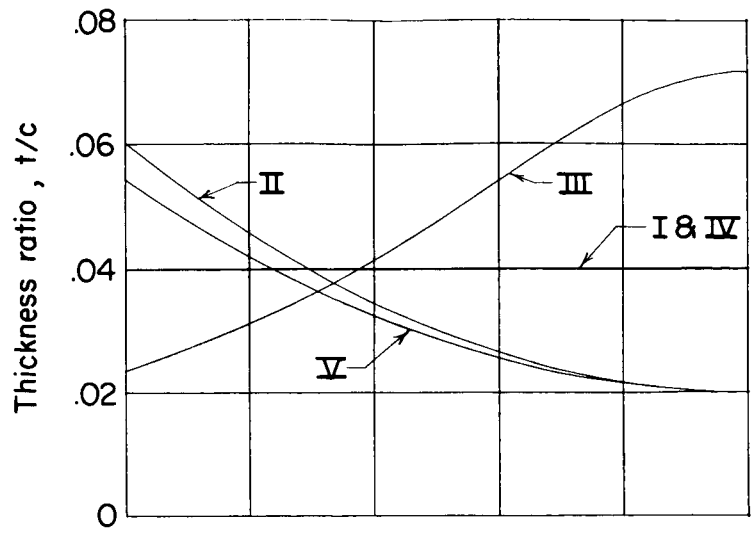
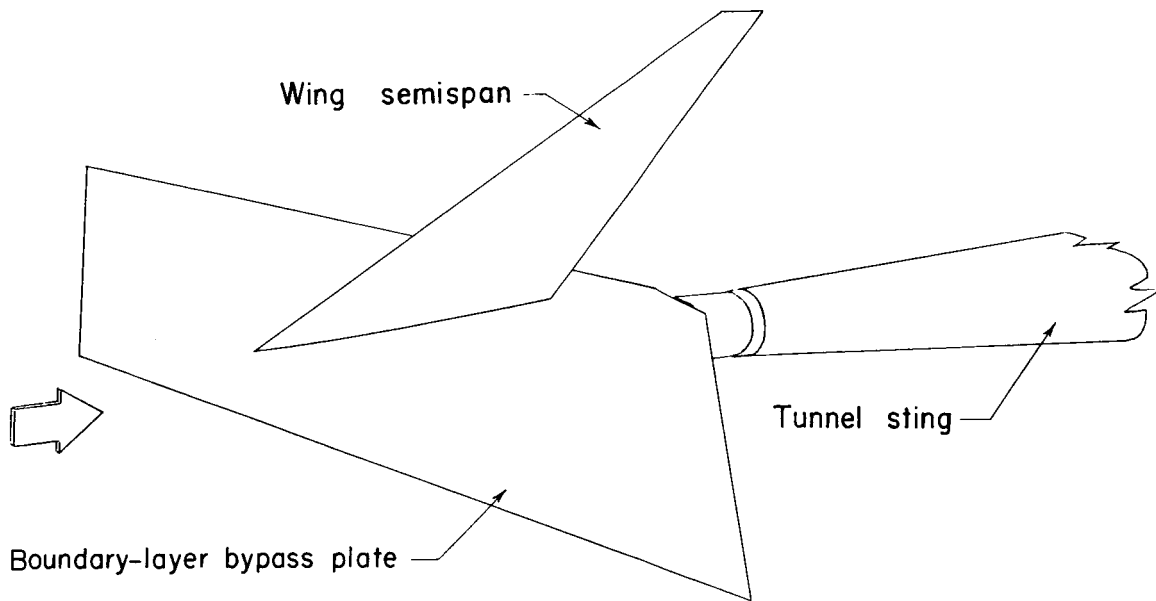
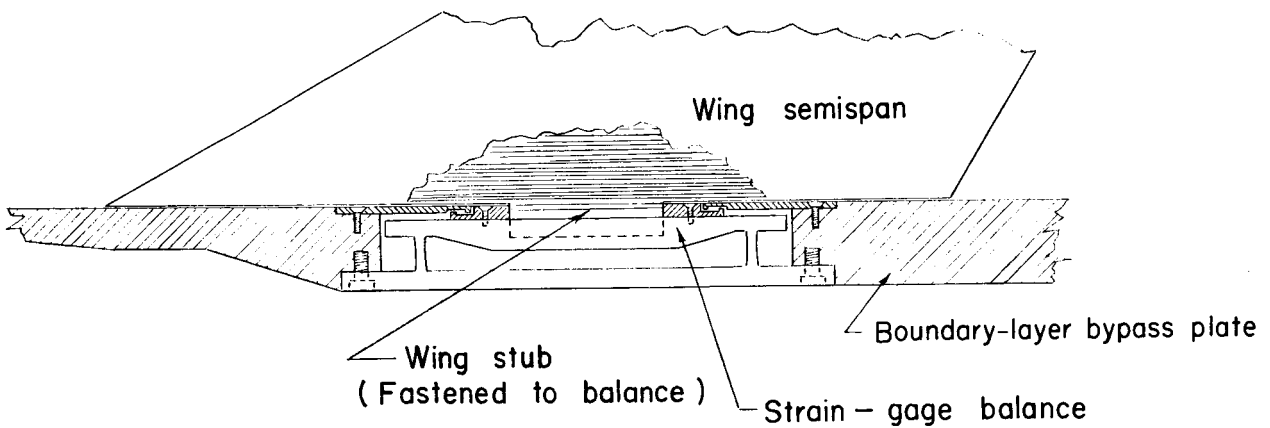


Figure 2.- Spanwise development of thickness ratio and volume for all wings of the series.



(a) Test rig in tunnel. Upper surface of boundary-layer bypass plate is parallel to tunnel flow.



(b) Plate-balance-model details.

Figure 3.- Sketch of test setup.

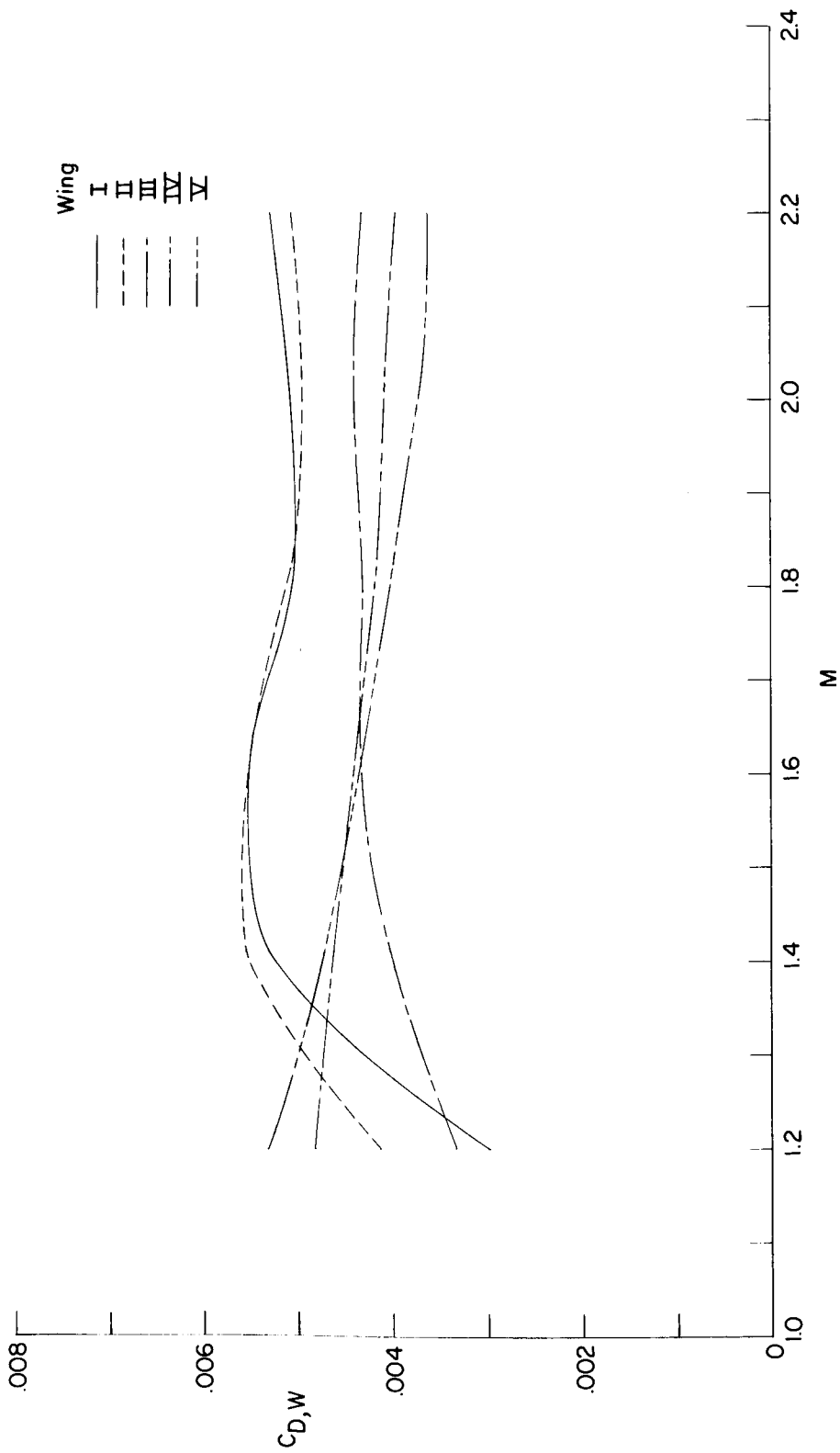
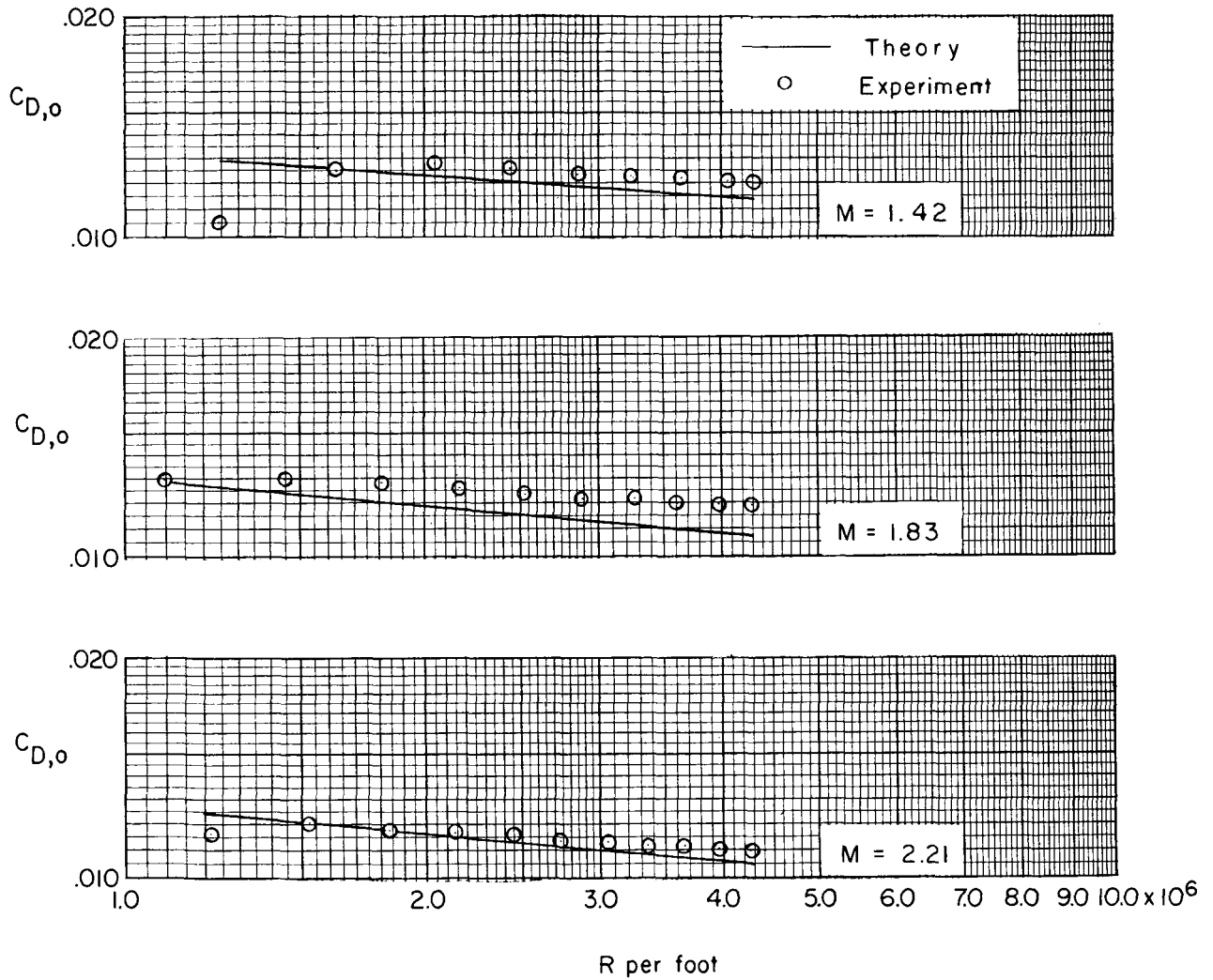
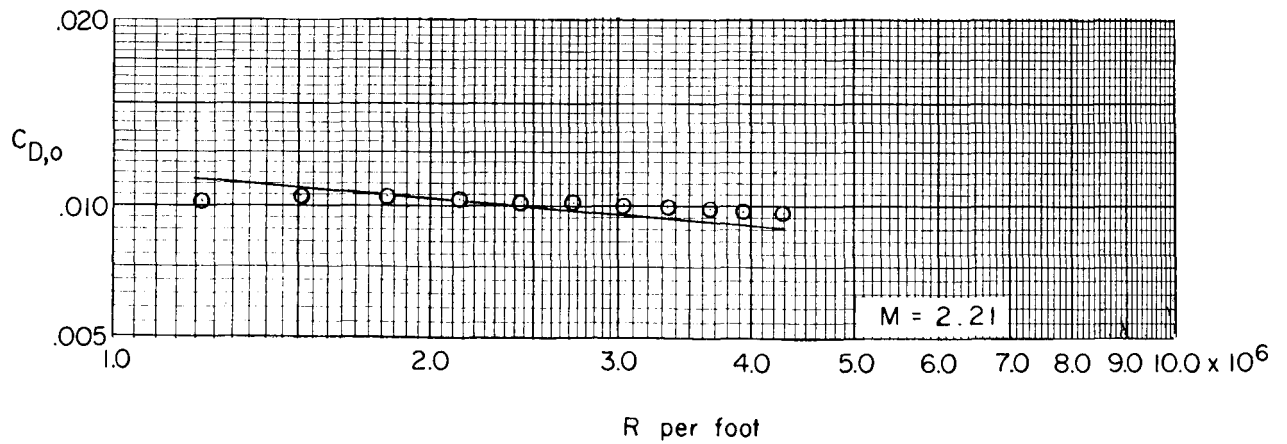
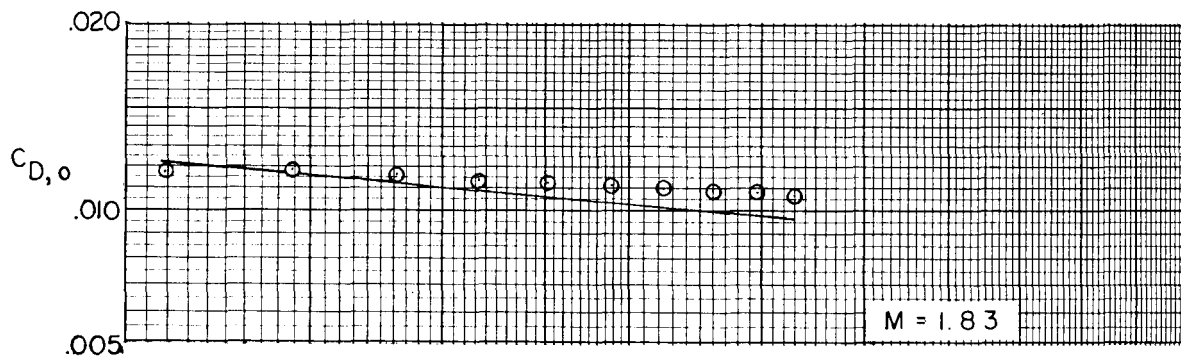
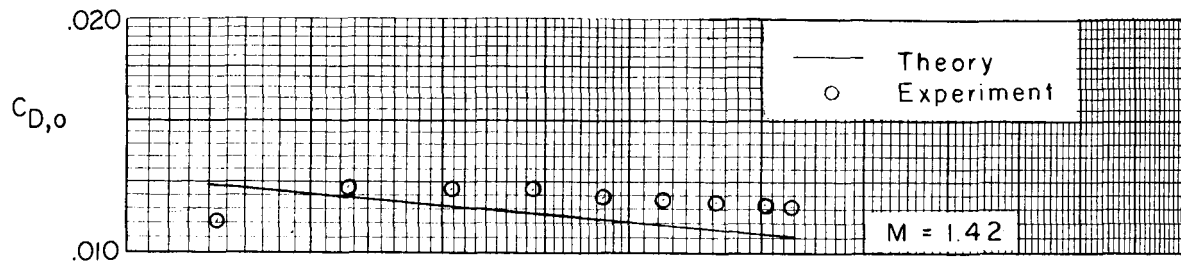


Figure 4.- Variation of theoretical zero-lift wave drag coefficient with Mach number for all wings.



(a) Wing I.

Figure 5.- Variation of zero-lift drag coefficient with Reynolds number.



(b) Wing IV.

Figure 5.- Concluded.

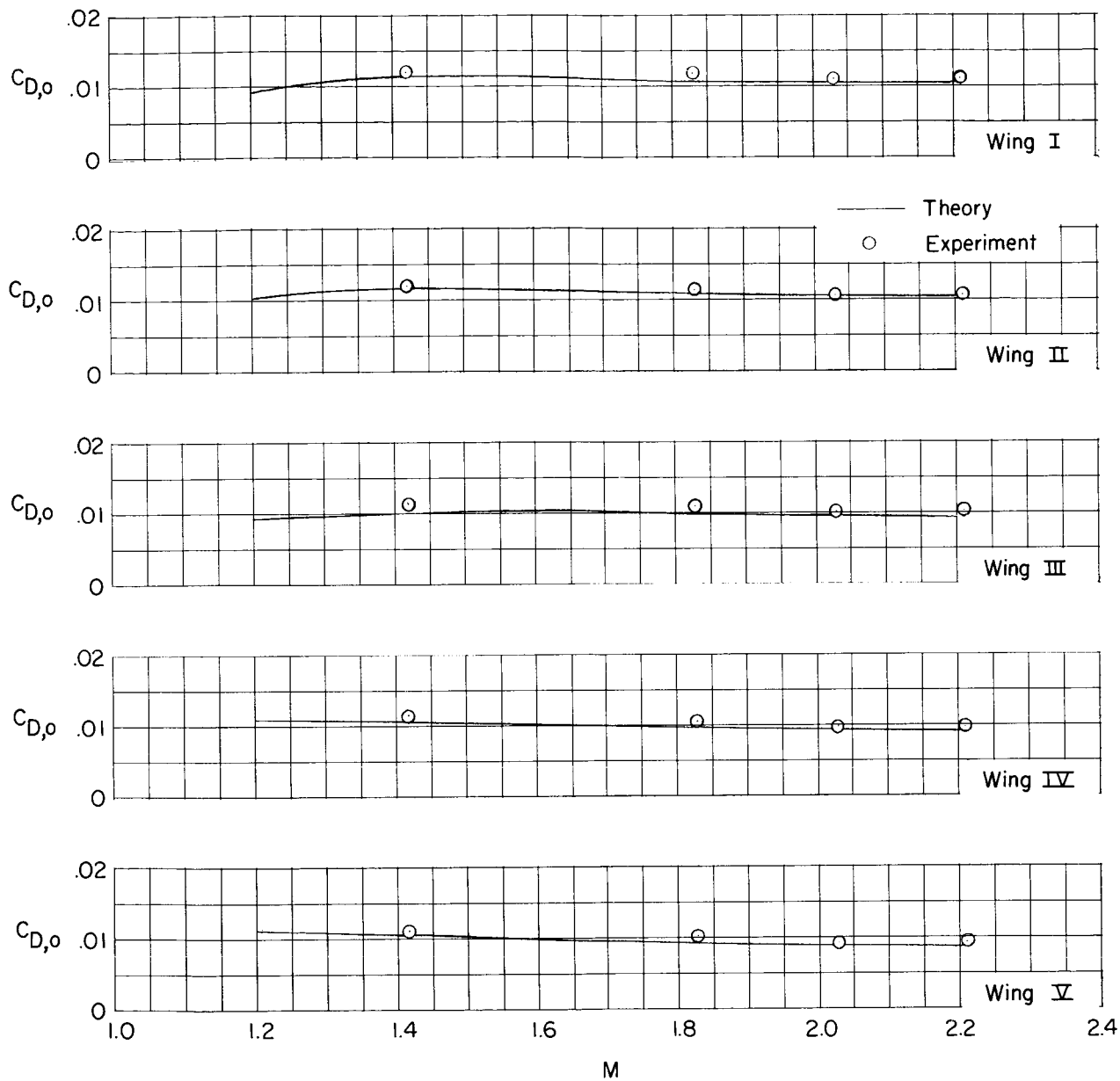


Figure 6.- Variation of zero-lift drag coefficient with Mach number for the wing family.
 $R = 4.3 \times 10^6$ per foot.

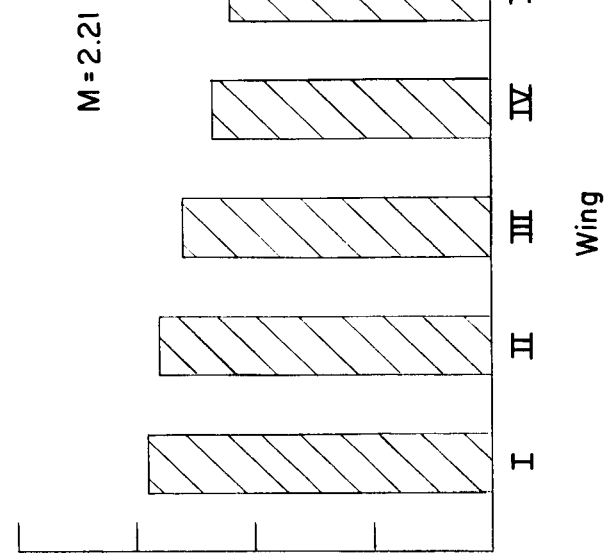
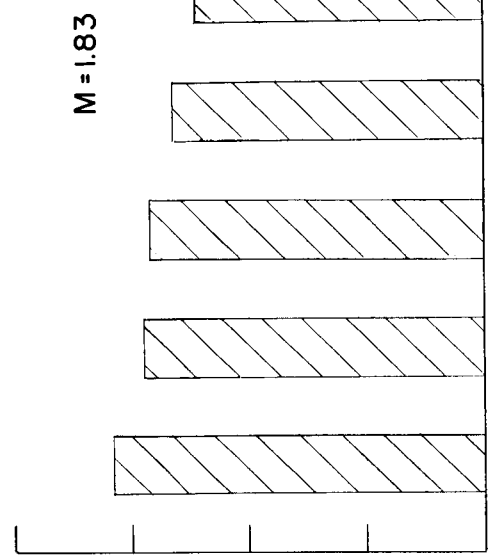
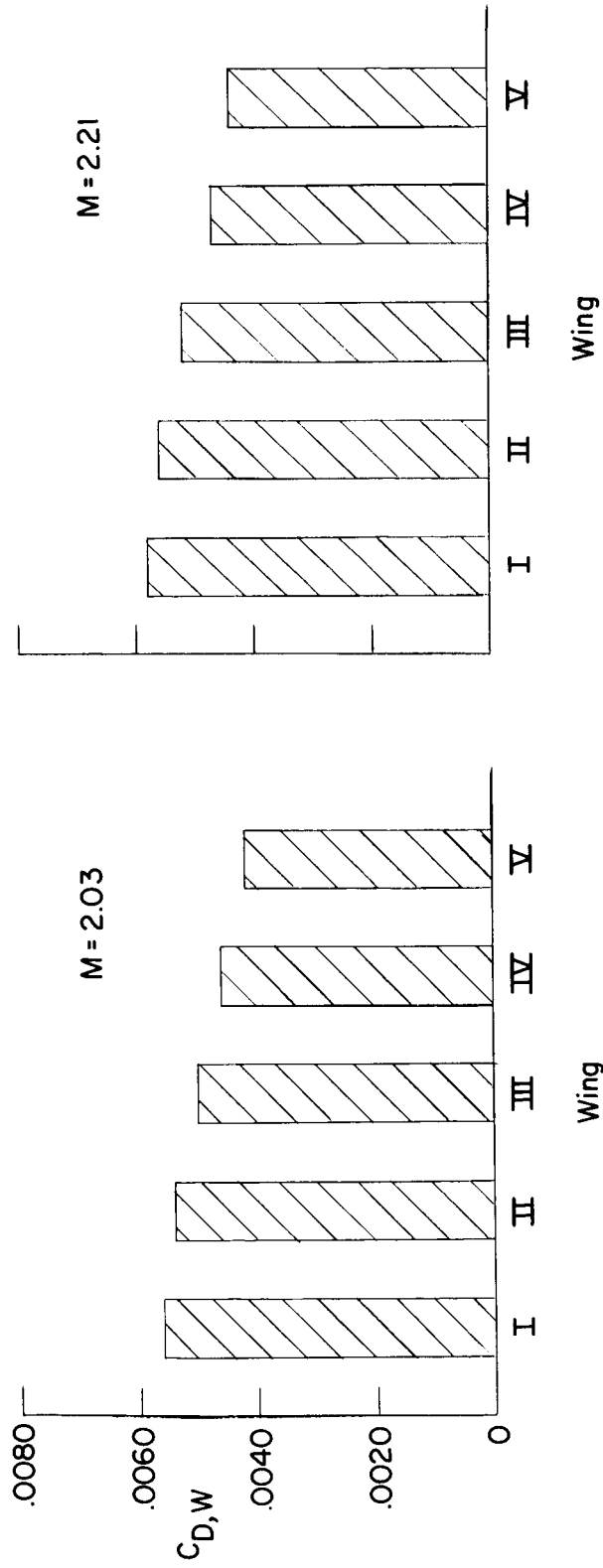
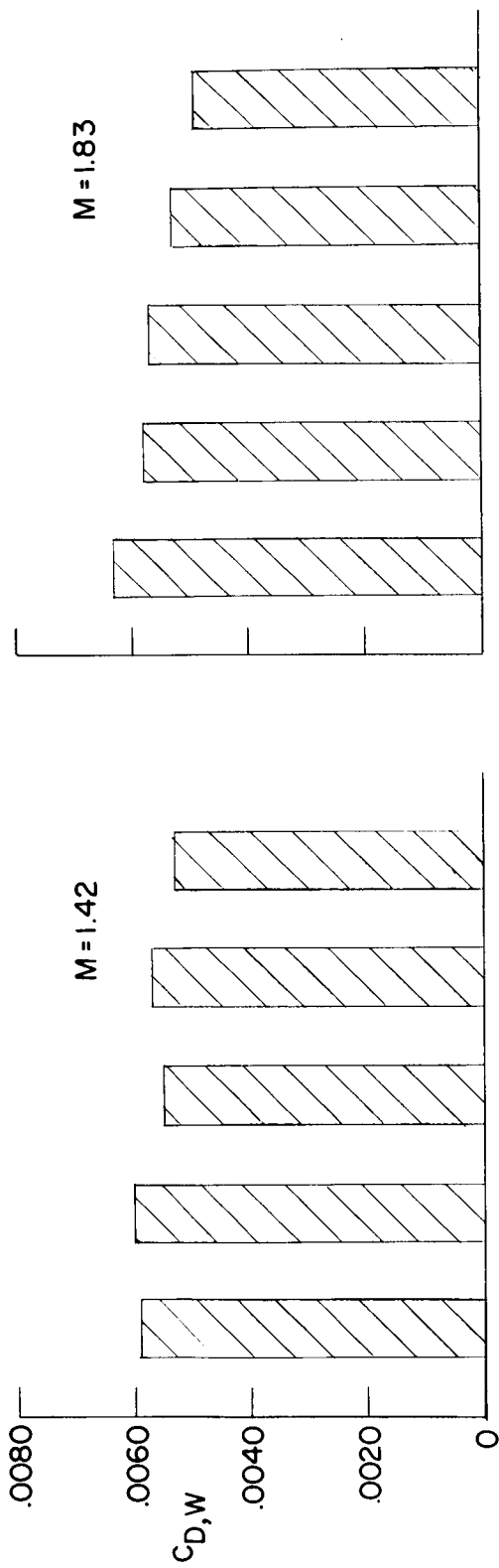


Figure 7.- Experimental zero-lift wave drag coefficients for the wing family at various Mach numbers.

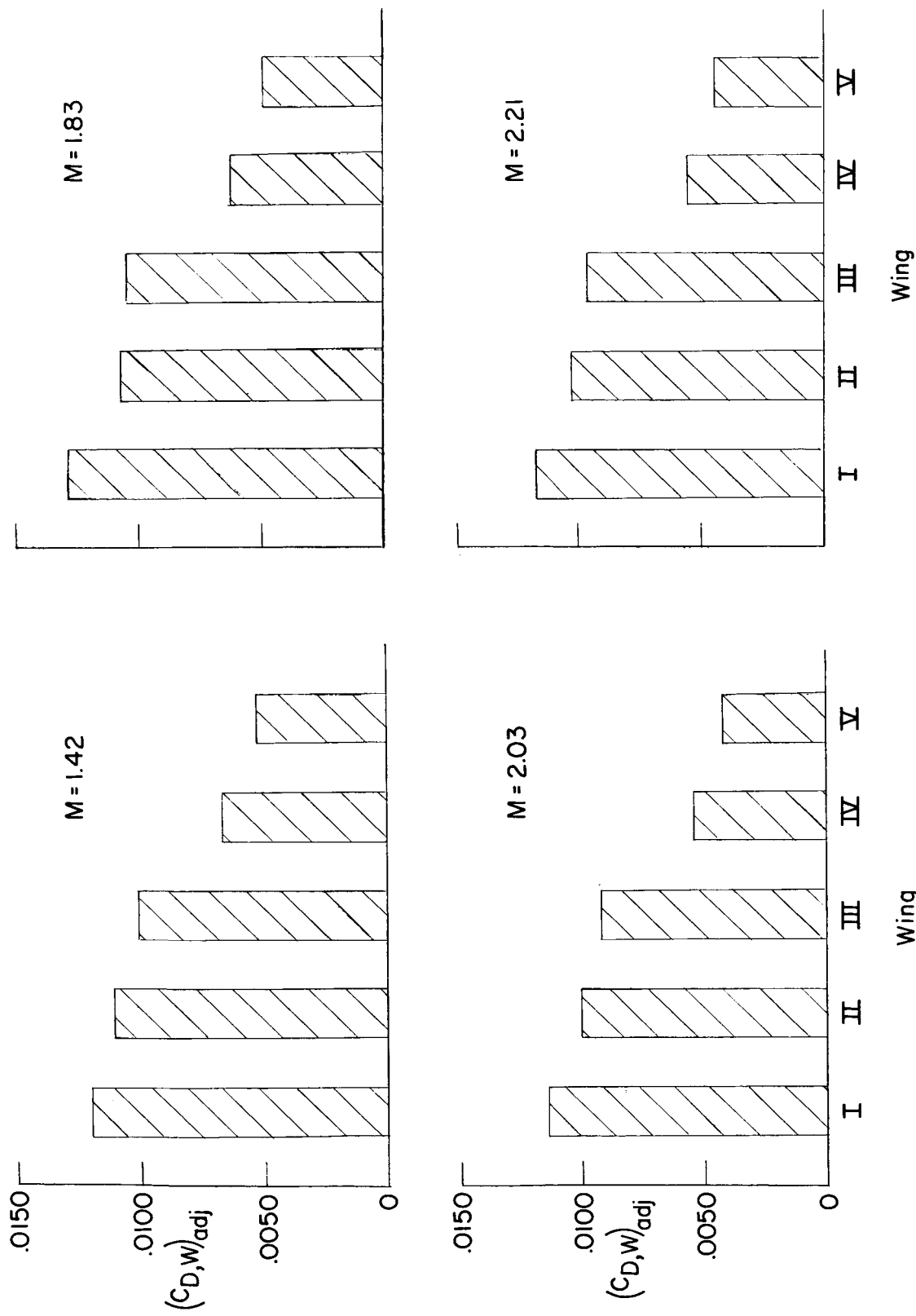


Figure 8.- Zero-lift wave drag coefficients adjusted on the basis of equal volume for each wing.

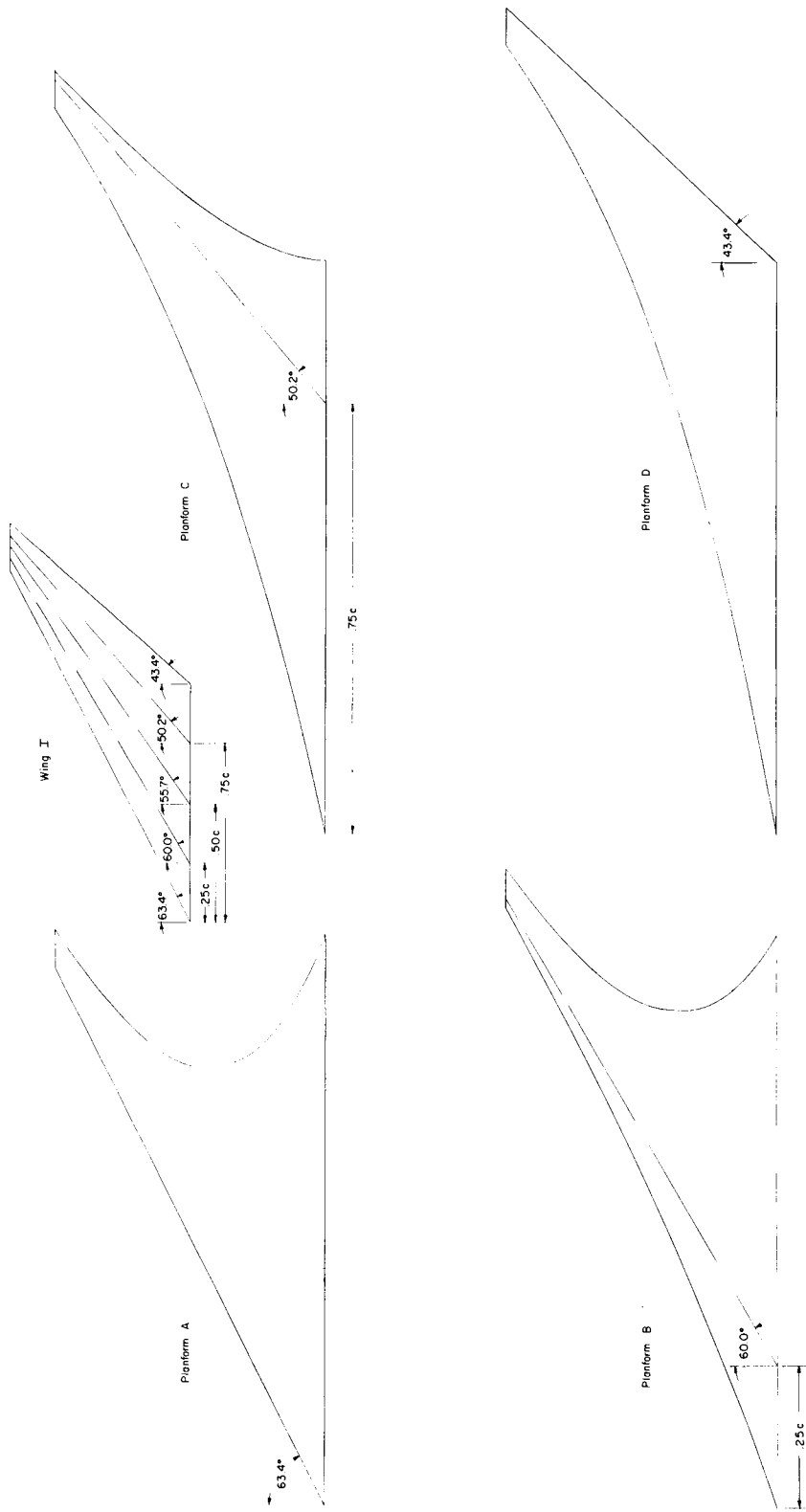
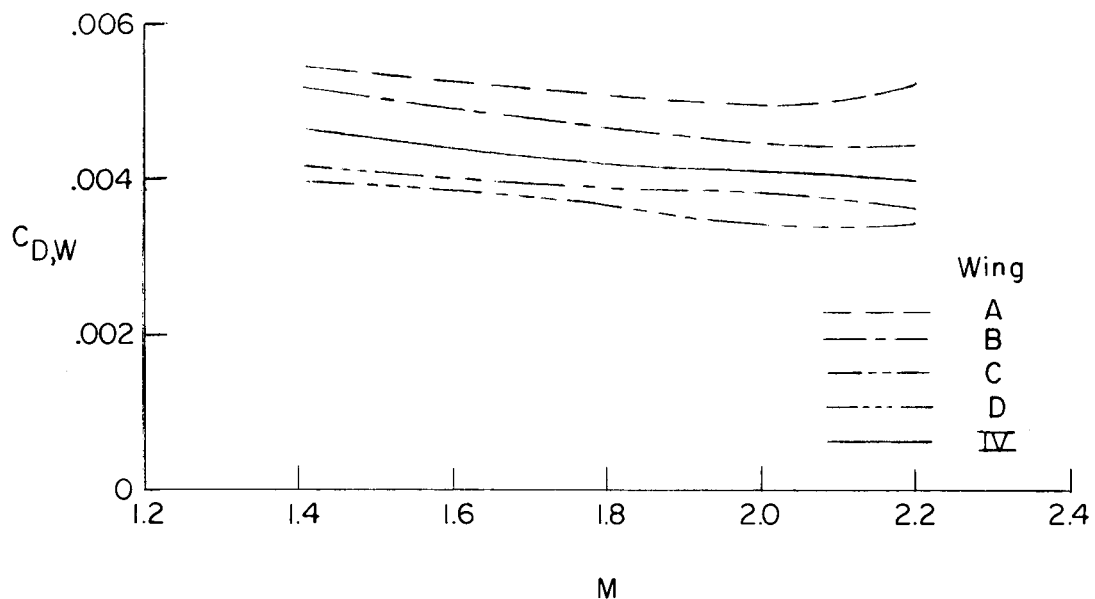
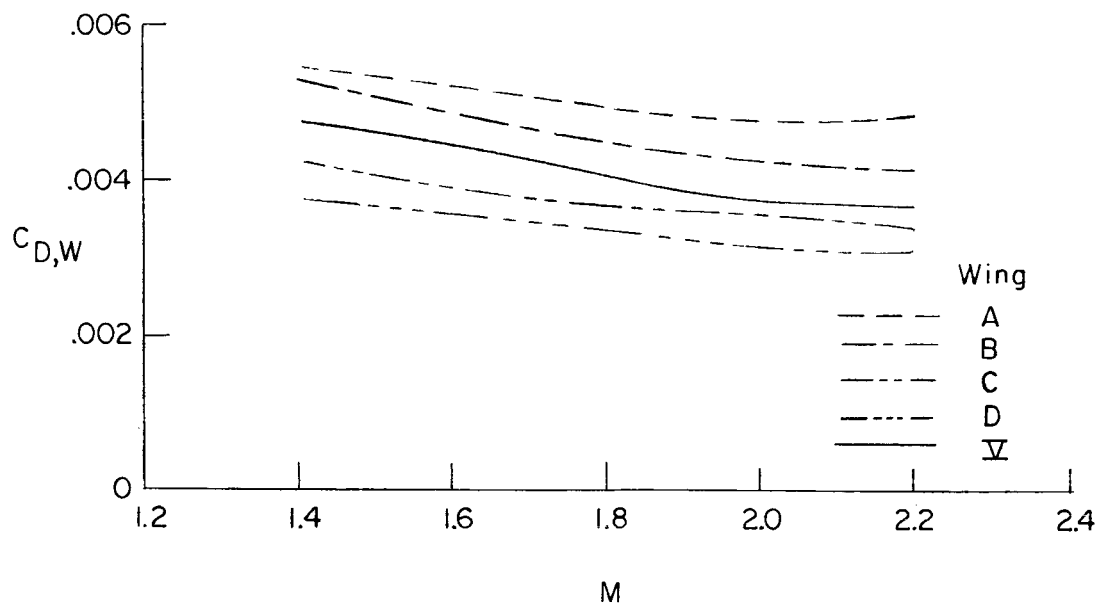


Figure 9.- Sketches of planforms of the two series of wings derived from original family.



(a) Wing series with thickness distribution of wing IV.



(b) Wing series with thickness distribution of wing V.

Figure 10.- Theoretical zero-lift wave drag variation with Mach number for the derived wing series.